Corresponding Author: Mr. Henk Versteeg,

Corresponding Author's Institution: Loughborough University

First Author: Affaro Affandy, PhD Biochemical Engineering

Order of Authors: Affaro Affandy, PhD Biochemical Engineering; Eli Keshavarz-Moore, PhD Biochemical Engineering; Henk K Versteeg, MEng Mechanical Engineering

Abstract: Sterile filtration is considered as a final step in processing pharmaceutical grade plasmid DNA. During the development of the filtration process, fundamental understanding on the mechanism of fouling is critical to improve filtration operations. The mechanism of fouling of pQR150 (20 kb) and pGEc47 (56 kb) plasmids DNA during constant pressure filtration inside 0.22 μm PVDF membrane is experimentally investigated. The decline of filtrate flux as function of time is analysed using the framework of classical and combined blocking models. The results for both plasmids indicate a transition between fouling mechanisms. Initially, during early part of the filtration, the intermediate blocking model provided the best fit of the experimental results suggesting that fouling of the membrane was mainly caused by deposition of particles onto its surface. Afterwards, the result trends were best captured by the standard blocking model indicating that internal fouling of membrane was the dominant fouling mechanism. A study of the transmission (C_f/C_0) of both plasmids shows a significant reduction of plasmid transmission which coincides with the transition of the fouling mechanism from intermediate to standard blocking. The study highlights how the fouling behaviour of large plasmid DNA during sterile filtration is determined by the complex interplay between the flexibility of the molecules and the internal structure of the membrane.

1

Application of filtration blocking models to describe fouling and transmission of large plasmids DNA in sterile filtration

Affaro Affandy[1,3], Eli Keshavarz-Moore[1], Henk K. Versteeg[2†]

[1]The Advanced Centre for Biochemical Engineering, University College London, Torrington Place, London WC1E 7JE, United Kingdom. [2]Healthcare Engineering, Wolfson School of Mechanical and Manufacturing Engineering, Loughborough University, Loughborough, United Kingdom. [3]Department of Biotechnology, Kuliyyah of Science, International Islamic University Malaysia, Malaysia.

10   _____

Abstract

Sterile filtration is considered as a final step in processing pharmaceutical grade plasmid DNA. During the development of the filtration process, fundamental understanding on the mechanism of fouling is critical to improve filtration operations. The mechanism of fouling of pQR150 (20 kb) and pGEc47 (56 kb) plasmids DNA during constant pressure filtration inside 0.22 µm PVDF membrane is experimentally investigated. The decline of filtrate flux as function of time is analysed using the framework of classical and combined blocking models. The results for both plasmids indicate a transition between fouling mechanisms. Initially, during the early part of the filtration, the intermediate blocking model provided the best fit of the experimental results suggesting that fouling of the membrane was mainly caused by deposition of particles onto its surface. Afterwards, the result trends were best captured by the standard blocking model indicating that internal fouling of the membrane was the dominant fouling mechanism. A study of the transmission of both plasmids shows a significant reduction of plasmid transmission which coincides with the transition of the fouling mechanism from intermediate to standard blocking. The study highlights how the fouling behaviour of large plasmid DNA during sterile filtration is

[†]Corresponding author. Email address: h.k.versteeg@lboro.ac.uk

1 determined by the complex interplay between the flexibility of the molecules and the internal

2 structure of the membrane.

3 Keywords: Sterile filtration, plasmid DNA, fouling, blocking models, filtration law

4 **1. Introduction**

5 Current progress in gene therapy and DNA vaccination has increased demand for and interest

6 in plasmid DNA. At present, four DNA vaccine and gene therapy products have been licensed

7 for veterinary use [1]. The processing of non-viral DNA for gene therapy and vaccination has

8 been reviewed widely and this involves several unit processes [2-6]. This article is focused on

9 the sterile filtration step which typically constitutes one of the final stages in the production of

10 therapeutic grade DNA. While there is general consensus that the study of this processing step

11 is of paramount importance, relatively little systematic work has been done in the area. A

12 particular concern is the issue of product loss related to fouling of the membrane. A recent study

13 by Kong et al (2006) [7] has shown that plasmid filtration through 0.22 µm filter resulted in

14 losses of up to 80% for 116 kb naked DNA. The result suggested an increase of losses of DNA

15 when the molecular size of plasmid increases.

16 At present, small plasmids (less than 20 kb) have been used in gene therapy and DNA

17 vaccination. The application of large plasmids may become critical in the future to enable

18 specific therapeutics applications which require large pieces of genetic information. Examples

19 are the demand of multi-genes for certain therapeutic purposes and incorporation of cytokines

20 for the enhancement of immune response of encoded antigens [8].

21 Fouling is the blockage or retention of impurities or product of interest onto the surface of or

22 inside the membrane. It affects the quality and transmission of the desirable product. One of

23 strategies to investigate these interactions is by direct visualisation method using various

2

1 microscopy techniques [9-11]. However, microscopy techniques are unable to supply real time

2 information of the filtration process. Besides the preparation of samples is labour intensive and

3 time consuming.

4 The progress of fouling during constant pressure filtration can also be characterised by

5 mathematical analysis of flux decline during filtration. By employing filtration blocking models,

6 firstly the mechanism of fouling and secondly the transition of the progress of fouling in the filter

7 can be determined. Conventional filtration blocking models have been widely applied to

8 investigate fouling mechanisms and to predict the capacity of membranes which is critical for

9 filter scale-up. Four classical filtration models describe the mechanism of fouling during particle

10 filtration through the following mechanistic models: (i) standard blocking (gradual pore

11 constriction), (ii) complete blocking (sealing of pore entrances), (iii) intermediate blocking

12 (sealing and accumulation on membrane surface) and (iv) cake filtration blocking models [12].

13 Combinations of these models were later developed to account for more complex fouling

14 mechanisms during filtration [13-15]. Table 1 summarises the equations governing the filtrate

15 volume collected as a function of time for each model. In these equations, V is the filtrate

16 volume (m^3), V_0 is the initial volumetric flow rate (m^3/s), A_0 is the initial membrane frontal area

17 (m^2), t is time (s) and k_s, k_i, k_b, k_c and k_{ic} are fouling parameters.

Models	Equations	Fouling parameter
Standard blocking [16]	$V = (V_0 t)\left(1 + \dfrac{k_s V_0}{A_0} t\right)^{-1}$	k_s (m^{-1})
Intermediate blocking [16]	$V = \dfrac{1}{k_i} \ln(1 + k_i V_0 t)$	k_i (m^{-3})
Complete blocking [16]	$V = \dfrac{V_0}{k_b}\left[1 - \exp(-k_b t)\right]$	k_b (s^{-1})
Cake filtration [16]	$V = \dfrac{1}{V_0 k_c}\left(\sqrt{1 + (2 k_c V_0^2 t)} - 1\right)$	k_c (s.m^{-6})
Intermediate-standard [13]	$V = \dfrac{A_0}{k_{ic}} \ln\left(1 + \dfrac{2 k_{ic} (V_0/A_0) t}{2 + k_s (V_0/A_0) t}\right)$	k_{ic} (m^{-1}) and k_s (m^{-1})
Complete-standard [13]	$V = \dfrac{V_0}{k_b}\left(1 - \exp\left(\dfrac{-2 k_b t}{2 + k_s (V_0/A_0) t}\right)\right)$	k_b (s^{-1}) and k_s (m^{-1})

1 Table 1- Summary of classical and combined blocking models for constant transmembrane pressure

2 filtration

3 In cases where transition of fouling and the operative particle retention mechanisms take place

4 during filtration, this can be estimated by using the following mathematical form [14, 17, 18]:

$$\frac{d^2t}{dV^2} = k\left(\frac{dt}{dV}\right)^n \qquad \text{Equation 1}$$

1   Equation 1 expresses the rate of variation of the instantaneous resistance to filtration in term of

2   a power law function of the instantaneous resistance. The parameter k in Equation 1 is the

3   filtration constant. The exponent n characterises the fouling mechanism; it can be shown that

4   n=0 corresponds to cake filtration, n=1 for intermediate blocking, n=1.5 for standard blocking

5   and n=2 for complete blocking [12]. Changes to the value of n during filtration indicate more

6   complex fouling mechanisms that are more accurately captured by one of the combined models.

7   The investigation of the mechanism of fouling is important in defining optimum filtration

8   condition; in terms of process parameters, product-membrane interactions and optimisation of

9   numerous membrane attributes such as pore architecture. The filtration blocking model is also

10   applied to predict the maximum volumetric capacity (V_{max}) of a membrane [15, 19]. Therefore,

11   an accurate determination of the specific model that describes the fouling mechanism leads to

12   better sizing prediction during scaling up of filtration.

13   Before we can apply the filtration blocking models, it is important to understand the dominant

14   fouling mechanism. However, the above models have their limitations due to inherently simple

15   assumptions relating to the filter and particulate characteristics. The filter is assumed to consist

16   of cylindrical pores whereas actual membranes exhibit highly interconnected, tortuous flow

17   passages [15]. The feed is assumed to contain a suspension of hard spherical particles, but

18   plasmid DNA molecules considered in this study are flexible and coiled shape structure.

19   Furthermore, the conformation and orientation of plasmids in liquid solution is dynamic and

20   influenced by fluid flow [20, 21]. Therefore the ability of these models to explain the filtration

21   behaviour of plasmid DNA, especially large plasmids, needs to be studied.

This paper reports the findings of an investigation of the sterile filtration of two large plasmids DNA- pQR150 (20 kb) and pGEc47 (56 kb) during constant pressure filtration with a 0.22 μm PVDF membrane. Analysis of the flux decline using filtration blocking models provides information on the specific fouling mechanism that dominates the fouling during the entire course of filtration. The transmission (C_f/C_0) of the plasmids was studied in an attempt to understand the connection between transmission characteristics and flux decline. The results enable us to comment on the applicability of filtration blocking model to explain the fouling behaviour of large plasmid DNA during sterile filtration.

2. Materials and Methods

2.1   Plasmid and bacterial cultures

Plasmids pQR150 (Kanamycin resistance, 20 kb) and pGEc47 (Tetracycline resistance, 56 kb) were used in this experiment and grown in E.coli DH5α and DH1 respectively. The bacteria were grown on plates containing Nutrient Broth (Oxoids, Basingstoke, Hertfordshire, UK) with appropriate antibiotic. A single colony of bacteria was selected and inoculated to seed cultures of 10, 50, 100 and 500 ml. The media based on Wubbolts et al [22] was used as fermentation medium for E.coli DH1 and Nutrient Broth was used to grow the DH5α.The cultures were grown at 37^0C for 8 hours with vigorous shaking (200 rpm) for subsequent fermentation.

5 and 10 litres working volume fed-batch fermentation of bacteria was grown with the BioFlow 310 fermenter (New Brunswick, Cambridge, U.K) and Applikon 20 litres bioreactor (Applikon Biotechnology, Gloucestershire, U.K) with addition of 0.2 % w/v dextran and trace elements. A pH of 6.3 ± 0.2 was maintained by automatic pumping of 1 M sodium hydroxide (NaOH) and 1 M phosphoric acid (H_3PO_4). Dissolved Oxygen was maintained at 30% by automatic stirrer

1 speed adjustment. To avoid foaming during fermentation, polypropylene glycol (50% v/v) was

2 added as an antifoaming agent.

2.2 Purification of plasmid DNA

4 E. coli cells were harvested from fermentation media by Beckman J2-M1 centrifuge (Beckman-

5 Coulter, High Wycombe, U.K) for 30 minutes at 4000 rpm. The cell paste was then stored at -

6 20ºC for further use. For purification of plasmid DNA, the cells were dissolved with resuspension

7 buffer (Buffer P1) containing 50 mM Tris-Cl (pH 8), 10 mM EDTA and 100 µg/ml RNase A. The

8 cells were then treated with lysis buffer containing 200 mM NaOH and 1% SDS (Buffer P2) for

9 2-5 minutes. The mixture was mixed gently to degrade the bacteria cell wall and to avoid

10 degradation of SC plasmids DNA. Neutralising buffer containing 3.0 M potassium acetate pH

11 5.0 (Buffer P3) was then added to precipitate proteins and other contaminants. The alkaline

12 lysis buffers P1, P2 and P3 were supplied by Qiagen (Qiagen, West Sussex, U.K). The mixture

13 was centrifuged for 5 minutes at 4000 rpm and subsequently filtered using 47 mm grade 4 (20-

14 25 µm pore size rating) cellulose filters (Whatman, Kent, U.K). The plasmid was later purified by

15 Hispeed Tip^{TM} anion exchange column chromatography and Qiaprecipitator^{TM} of Qiagen

16 Hispeed plasmids purification kits (Qiagen, West Sussex, U.K). The plasmid was then eluted

17 with 10 mM Tris-EDTA buffer.

2.3 Agarose gel electrophoresis

19 The plasmid DNA isoforms were confirmed by agarose gel electrophoresis. 0.6 % agarose gel

20 was pre-stained with 0.5 µg/ml final concentration of ethidium bromide. The gel was run in 1X

21 Tris-Borate EDTA (Sigma Aldrich, Dorset, UK) at 4.5 volts/cm for 4 hours. Supercoiled DNA

22 ladder (Invitrogen, Paisley, U.K.) and BAC DNA ladder (Epicentre Biotechnologies, Cambridge,

1 UK) were used to determine the size of plasmids. Images of the DNA bands were acquired and

2 processed with Gel Doc[TM] EQ gel documentation system and Quantity One[TM] gel analysis

3 software (BioRad, CA, USA). The unfiltered feed solutions of pQR150 plasmid (20 kb) had a

4 typical supercoiled (SC) content of > 80%. For pGEc47 plasmid (56 kb), the SC content of

5 unfiltered feed solutions was > 50 %.

6 ## 2.4   Spectrophotometry analysis

7 The concentration of DNA was measured using NanoDrop[TM] 2000 spectrophotometer (Thermo

8 Scientific, DE, U.S). The purity of the DNA after purification was confirmed by analysis of

9 absorbance ratio at 260/280. The 260/280 ratio was used for determination of DNA purity

10 against protein contamination; the standard ratio for plasmid purity is 1.8-2.0.

11 ## 2.5   Filtration experiments

12 Normal flow filtrations were performed using a syringe filter unit equipped with sterilising grade

13 13 mm Millex[TM]/ Durapore® 0.22 μm polyvinylidene fluoride (PVDF) membrane (Millipore, MA,

14 USA). The filter unit was affixed to an Amicon Stirred Cell 8300 (Millipore, M.A., U.S) connected

15 to N_2 source. The pressure drop during the filtration was measured using Millipore Integrity Test

16 kits (Millipore, MA, US). The illustration of the filtration configuration is presented in Figure 1.

17 The plasmid DNA samples used in these experiments were pre-filtered with 0.22 μm membrane

18 before the constant pressure filtration at 5 and 8 psi transmembrane pressures. The total filtrate

19 volume for each filtration experiment is approximately 5 ml. All the experiments were performed

20 at room temperature.

1   The experimental data was acquired by collecting filtrate volumes in a specific time interval. The

2   filtrates were collected with collection tubes and an electronic balance was used to measure the

3   filtrate weight. The results shown in each plots are average of two or three experiments.
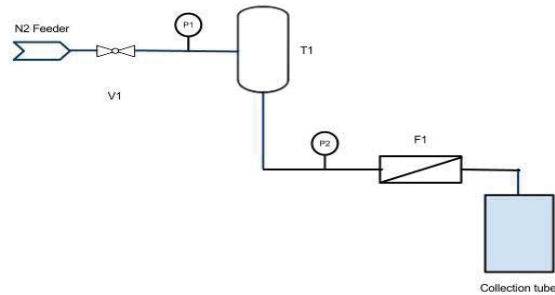
4

5   Figure 1- Illustration of a sterile filtration configuration. (V) valve, (P) pressure meter, (T) tank, (F) filter.

6   ## 2.6   Non-linear regression analysis

7   To analyse the fouling mechanism of plasmids pQR150 (20 kb) and pGEc47 (56 kb), the

8   experimental filtration data was initially fitted with the classical blocking models (standard,

9   intermediate, complete and cake filtration blocking models) using non-linear regression tool of

10   the SigmaPlot statistical and graphing package (Systat Software, London, U.K). The

11   experimental data was subsequently fitted with combined filtration blocking models developed

12   by Bolton et al (2006) [13] to determine whether the combination of classical models can

13   provide better fit with the experimental data. The non-linear regression works by minimizing the

14   sum of square residuals of the data points from the curve of the models.

15   ## 2.7   Power law fouling transition analysis

16   To investigate the transition of fouling mechanism during filtration, the filtrate flux data was

17   analysed in term of d^2t/dV^2 versus dt/dV as suggested in Equation 1. The derivatives dt/dV and

1 d^2t/dV^2 were computed by taking the analytical derivatives of the best fit functions (Table 1).

2 The values of dt/dV were obtained by reciprocal of the derivatives of filtrate volume vs. time plot

3 (dV/dt);

$$\frac{dt}{dV} = \frac{1}{dV/dt}$$
Equation 2

4 And the derivative of d^2t/dV^2 was obtained by:

$$\frac{d^2t}{dV^2} = \frac{d}{dV}\left(\frac{dt}{dV}\right) = \frac{dt}{dV} \times \frac{d}{dt}\left(\frac{dt}{dV}\right)$$
Equation 3

5 The power law coefficient, n was obtained by taking logarithms on both sides of power law

6 Equation 1 followed by a linear regression to yield the following form:

$$Log\left(d^2t/dV^2\right) = n * Log\left(dt/dV\right) + C$$
Equation 4

7 The average values of n during early, mid and late time of filtration of pQR150 (20 kb) and

8 pGEc47 (56 kb) plasmids at 5 and 8 transmembrane pressures was estimated using Equation

9 4.

10 The transformation of the values of n was then estimated by differentiating the logarithm of

11 d^2t/dV^2 with respect to the logarithm dt/dV:

$$n = \frac{d\left[\log\left(d^2t / dV^2\right)\right]}{d\left[\log\left(dt / dV\right)\right]}$$
Equation 5

12

2.8 Transmission analysis of filtrate

The transmission of plasmid during filtration is expressed by the ratio of DNA concentration of the filtrate over initial DNA concentration (C_f/C_0). The concentration of plasmid DNA was detected using the method explained in subsection 2.4. To obtain the concentration of filtrate at a specific time during the filtration, the filtrates were collected in batches. During the early stages of filtration (1-3 minutes) samples were collected every 10 seconds. Afterwards and towards the end of filtration samples were taken at 2 minutes intervals. This compensates for the low filtrate flux towards at the end of the filtration which requires sampling duration to increase.

3   Results and Discussion

3.1   Characterisation of plasmid DNA sample

The absorption property of DNA is used to assess the quality of plasmid DNA during the filtration. The absorbance ratio at A_{260}/A_{280} of both pQR150 and pGEc47 fall between1.8-2.0 which suggests acceptable purity of DNA against protein contamination. Furthermore, the absorbance ratio at A_{260}/A_{230} was also used as a secondary measurement of DNA purity against salts and organic compounds contamination. All samples used in this experiment fall within the acceptable range of A_{260}/A_{230} which is between 1.5-1.8. The characterisation of plasmid DNA samples using agarose gel electrophoresis showed that the plasmid is free from genomic DNA and RNA.

3.2   Analysis of fouling transition during filtration of plasmid DNA

In order to obtain understanding of the process of fouling, mathematical analysis has been performed to investigate the transition of fouling mechanism. Figure 2 illustrates the results of the power law analysis by means of log-log Equation 4. The slope of the line increases as log (*dt/dV)* increases, which corresponds to increasing time *t*. Since the slope of this line is equal to power law exponent *n* in Equation 1, the results indicate that a transition of the dominant fouling mechanism takes place during 8 psi transmembrane pressure filtration of pQR150 (20 kb) and pGEc47 (56 kb). A similar trend was observed during the filtration of both plasmids at 5 psi. The transition of the average value of *n* that describes the fouling behaviour during early, mid and late time filtration is extracted from these plots. Figure 3 contains information relating to the dominant fouling mechanism at a specific time during filtration in simplified form.

1 The common feature of all the results is that early on in the filtration, the exponent n originates

2 from a value that closes to 1. This implies that during this stage, intermediate blocking model

3 dominates the fouling, so plasmids are initially retained on the surface of membrane. Later on,

4 the values of n seem to approach $n \sim 1.5$ asymptotically. This value suggests that the fouling is

5 dominated by the standard blocking model where the internal fouling occurred within the depth

6 of the filter.

7 Figure 3 describes that during the filtration at 8 psi, the transition of the value of n (from low to

8 high n values) occurred earlier (at low dt/dV) for pQR150 (20 kb) than pGEc47 (56 kb). This is

9 expected since the smaller size of pQR150 (20 kb) allows the plasmid to penetrate the

10 membrane efficiently.

11
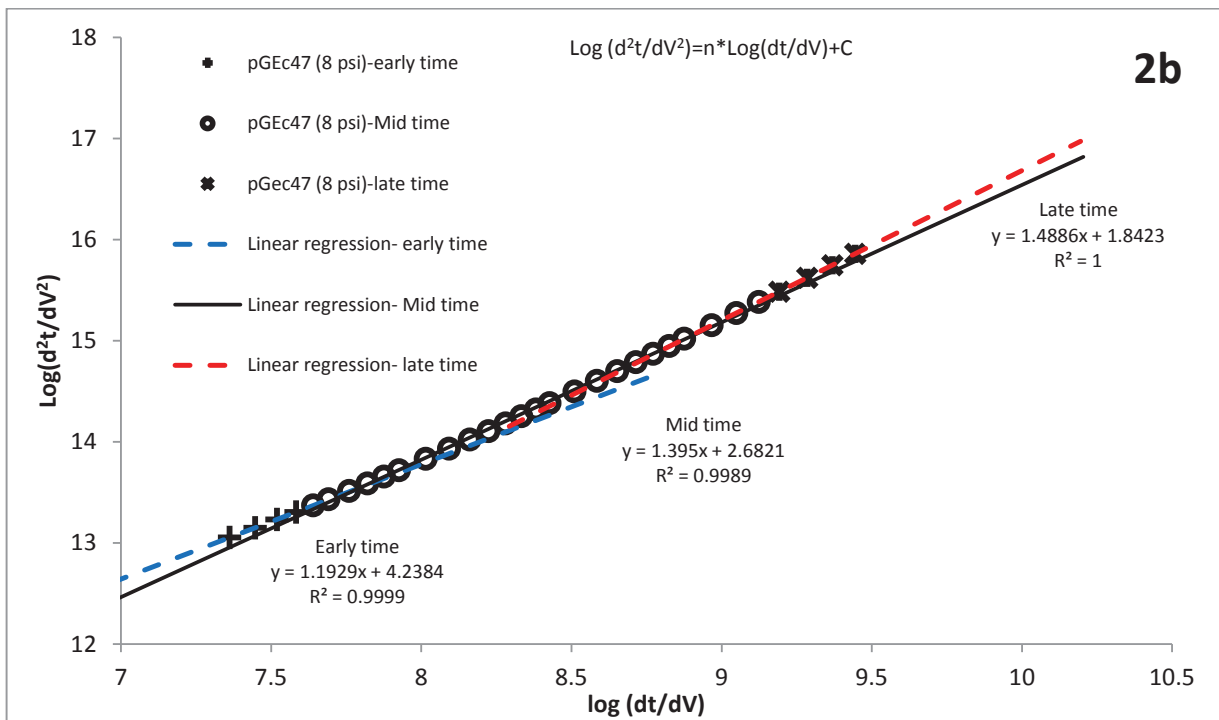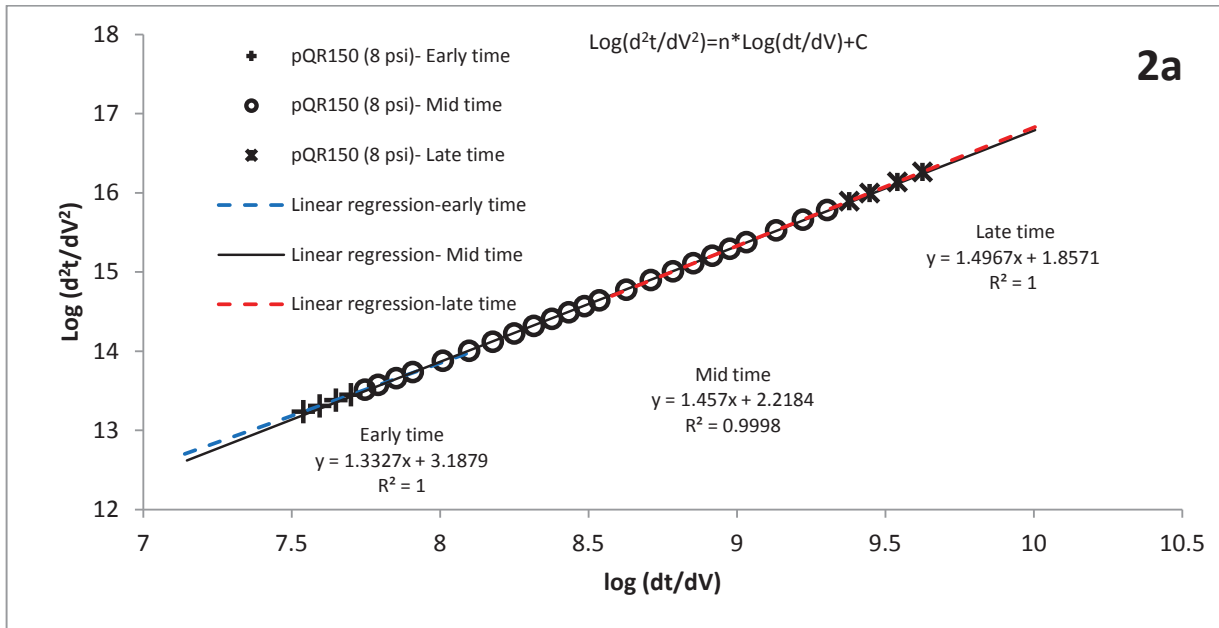
Figure 2- Flux decline analysis of pQR150 (20 kb) and pGEc47 (56 kb) filtrations at 8 psi transmembrane pressure.
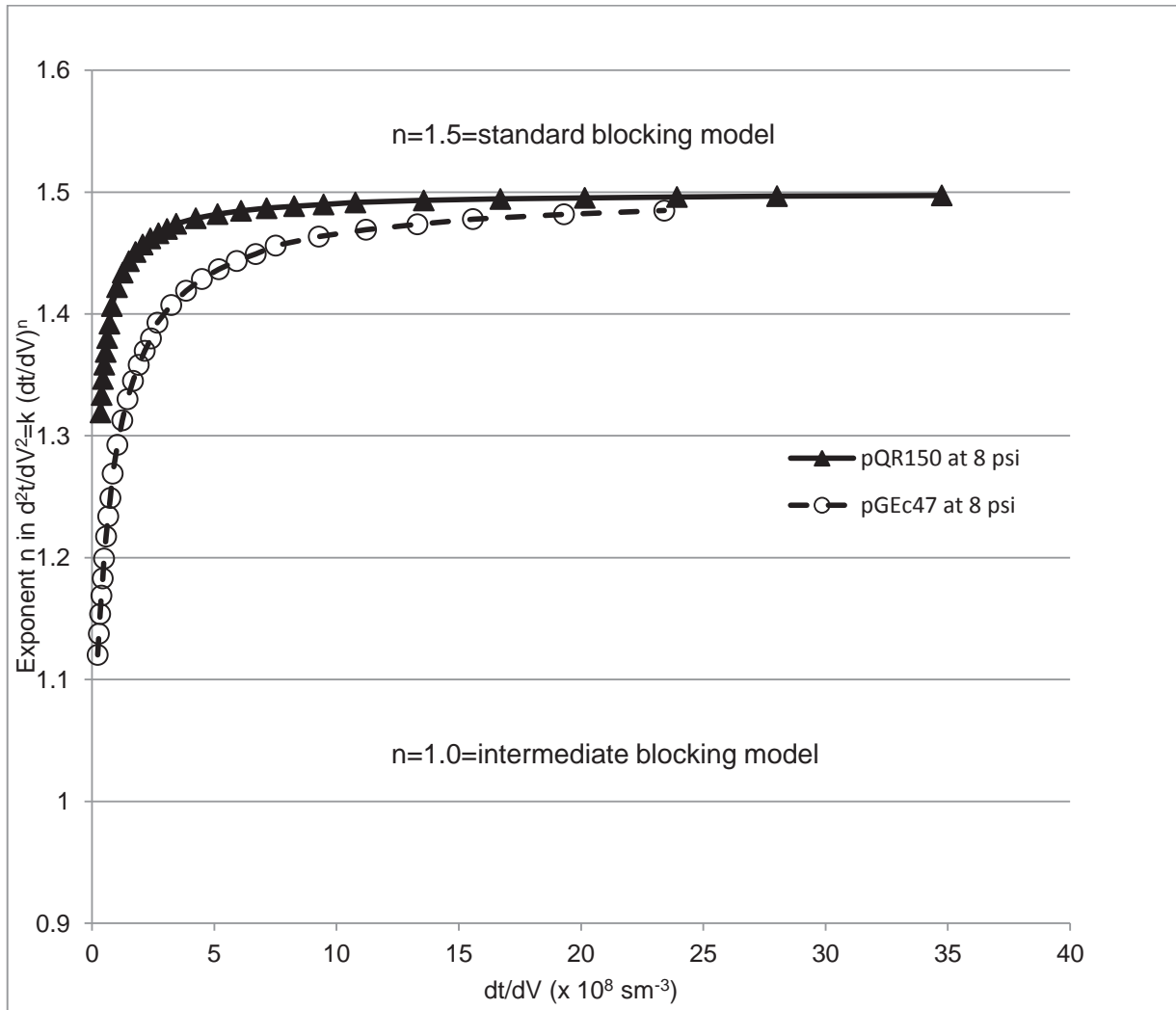
Figure 3 - The plot of exponent n (Equation 1) vs. dt/dV of the filtration of pQR150 (20 kb) and pGEc47 (56 kb) at 8 psi transmembrane pressure.

The filtration behaviour of DNA is different from protein and other particulates since DNA is a flexible long chain molecule. These characteristics allow DNA to penetrate the pores and elongate during the passage through the membrane. Furthermore, large DNA molecule with radii of gyration that is larger than the nominal pore size can potentially be retained inside the interstitial pore structure. It is possible that during its trajectory through the membrane,

1 entrapment of a plasmid occurs at the surface of pore and at the same time the other parts of a

2 plasmid penetrate along the web of the other pores.

3 The interesting feature of the present results is that the transformation of the values of n

4 contrasts with results observed during the microfiltration of particulate suspensions; such as

5 filtration of bovine serum albumin (BSA), which, like other proteins, can be successfully

6 modelled as rigid and sphere-shaped molecule [23]. BSA is a type of protein with a diameter

7 typically smaller than the nominal size of pores in microfiltration membrane [24]. Retention of

8 BSA was observed inside the inner wall of the pore and could be characterised using the

9 standard blocking model [25]. Other work has also shown that the fouling of BSA aggregates

10 occurred on the surface of membrane [26]. Iritani and co-workers [17] reported during the

11 filtration of BSA through 0.05 μm nitrocellulose membrane, the values of n were maximum at the

12 initial stage of filtration (low dt/dV) and decreased to 0 as the cake occurred at the end of

13 filtration.

14 Interestingly, during the filtration of pQR150 (20 kb) and pGEc47 (56 kb) plasmids, the values of

15 n increased with the increase of dt/dV until it approached asymptote around 1.5 that represents

16 the standard blocking mechanism. The value of n at early time filtration is close to 1; indicating

17 the intermediate blocking model dominated the fouling mechanism at this stage. The results

18 suggested that at the beginning of the filtration, plasmids DNA were trapped as its chain-like

19 molecule did not align with the surface of membrane. It is also thought that the trajectory and

20 orientation of plasmids is initially parallel with the surface of the filter. Since plasmids are

21 flexible, the molecule can realign its structure to penetrate the pore with the assistance of shear

22 stress originating from flow of the solution inside the membrane [27].

1   However, it should be noted that the usefulness of this analysis, i.e. the statistical precision of

2   the values of n in Figures 2 and 3 is strongly depends on the goodness of fit of the expressions

3   used in Table 1 and the original volume-time data. As explained in subsection 2.7, the

4   derivatives of dt/dV and $d^2t dV^2$ were computed by taking the analytical derivatives of the best fit

5   functions. It is worth to mention that small discrepancies between the volume-time data and the

6   best fit curve could amplify errors between actual derivatives of dt/dV and d^2t/dV^2. As our

7   interest is in the change of the power law constants, it is possible to control such errors to some

8   extent by repeating the best fit analysis on subsets of the data.

9   **3.3**   <u>**Analysis of fouling using classical filtration blocking models**</u>

10   The objectives of this study are to determine whether the classical filtration blocking models can

11   explain the fouling phenomena of large plasmids DNA and to find out the operative retention

12   mechanism of the fouling; i.e. whether a single or combination of fouling mechanisms exists.

13   In performing the non-linear regression, the initial volumetric flow rate, V_0 (m^3/s), initial

14   membrane frontal area; A_0 (m^2), and blocking constants; k_s, k_i, k_b, k_c, and k_{ic} are the required

15   constant parameters. The blocking constant was determined numerically while V_0 was obtained

16   from experiments and A_0 is based on specification supplied by the manufacturer. Therefore,

17   only one parameter was determined numerically by the software which is important to narrow

18   the confidence interval of the plots.

19   The flux decline analysis of d^2t/dV^2 vs. dt/dV shows that the values of n vary from ~1 to 1.5

20   which suggest that the transition of fouling is between intermediate (n=1) and standard (n=1.5)

21   blocking models. We only test these two models since the experimental data of n is neither

22   close to cake filtration (n=0) nor complete blocking model (n=2).

1   The experimental data were then fitted with standard and intermediate blocking models to

2   investigate the ability of these models to describe the flux decline phenomena during the

3   filtration of pQR150 (20 kb) and pGEc47 (56 kb) at 5 and 8 psi transmembrane pressures.

4   Figure 4 shows the experimental data and model predictions for pQR150 and pGEc47 at 5 and

5   8 psi transmembrane pressures.

6   Imperfect agreement between the predictions of the classical blocking models and experimental

7   data can be observed in Figure 4. The closeness of the model curves to the experimental data

8   was quantified by means of the standard error of estimates (Table 2).
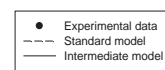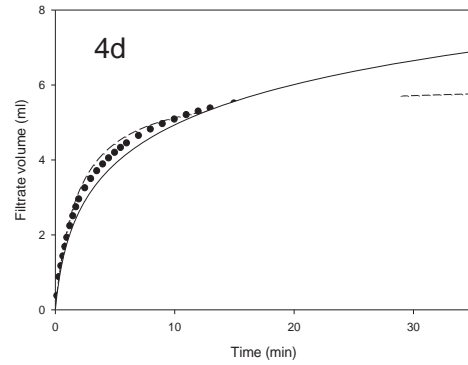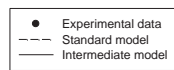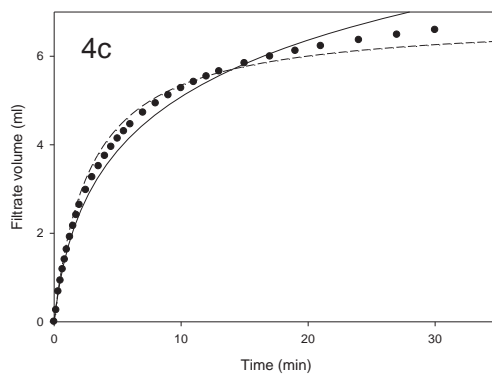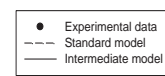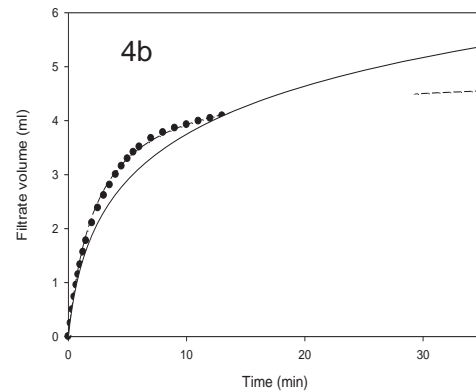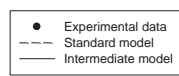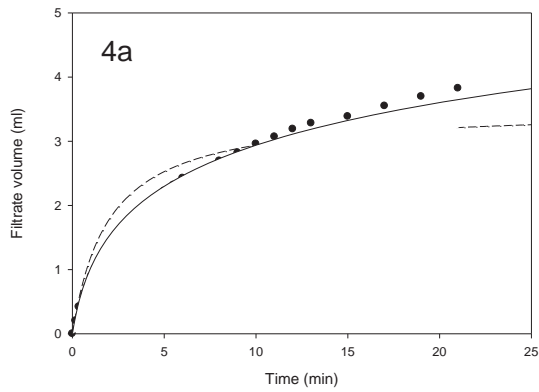
1

2

3   Figure 4 - Experimental data of filtrate volume vs. time fitted with the standard and intermediate blocking

4   models. Solution containing 50 µg/ml of plasmid was filtered through 0.22 µm PVDF membrane. Figure

5   4a represents pQR150 (20 kb) at 5 psi, 4b) pQR150 (20 kb) at 8 psi, 4c) pGEc45 (56 kb) at 5 psi and 4d)

6   pGEc47 (56 kb) at 8 psi transmembrane pressure.

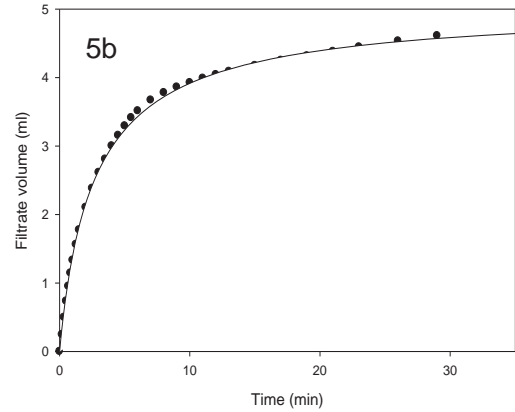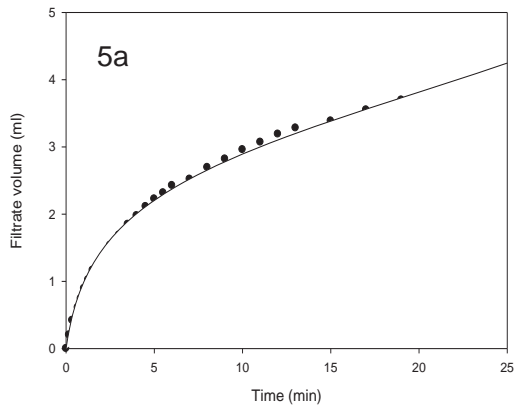| Plasmid	Model	Standard error of estimates 5psi transmembrane pressure	Standard error of estimates 8psi transmembrane pressure
pQR150	Standard	0.325	0.078
	Intermediate	0.120	0.272
pGEc47	Standard	0.191	0.342
	Intermediate	0.221	0.198

1   Table 2 - Standard error of estimates of the filtration of pQR150 (20 kb) and pGEc47 (56 kb) at 5 and 8

2   psi.

3   The results suggested that the classical blocking models were unable to describe the flux

4   decline during the entire course of filtration of pQR150 (20 kb) and pGEc47 (56 kb) plasmids as

5   intermediate or standard blocking models could only describe parts of the filtrate volume vs.

6   time (Figure 4). For example, the filtration of pQR150 (20 kb) at 8 psi transmembrane pressure

7   showed that the best fit occurred with the standard model during the first 20 minutes of filtration.

8   Furthermore, the best fit of the experimental data of pGEc47 (56 kb) occurred with intermediate

9   model but only for the first 5 minutes of filtration.

10   The results of the filtration of large plasmids (>20 kb) contrast with the filtration of small plasmid

11   (6 kb) which followed the standard blocking model with a very good fit of R^2>0.9999 [28]. The

12   mechanism of fouling of large plasmid DNA is different from the behaviour shown in smaller size

13   plasmid. Due to its smaller size, the latter will easily pass through the membrane as the plasmid

14   capable to align and deform more quickly into the direction of the flow, whereas large plasmid

15   DNA molecule has a higher tendency to deposit on the surface of membrane. This lends

16   support to the finding by Kong et al (2006) that the transmission of plasmids DNA depends on

17   its molecular weight [7].
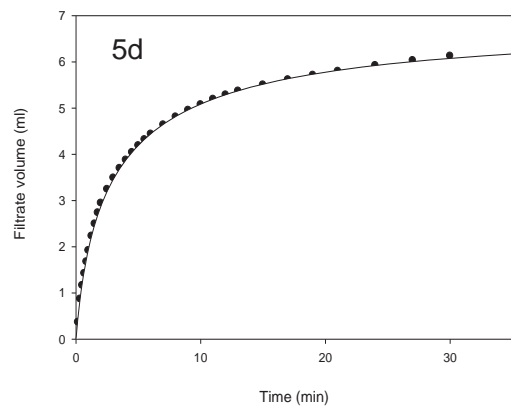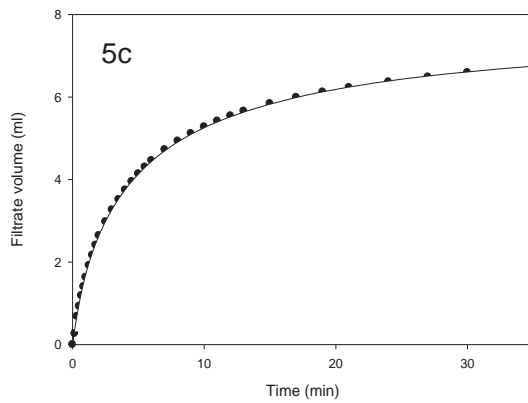
3.4   Analysis of fouling using combined blocking models

The test results suggested that the fouling mechanism of large plasmid DNA was not governed by a single fouling mechanism as described by the classical blocking models. Therefore, we tested the filtration data with the combined blocking models as described by Bolton et al. (2006); These authors discovered that the application of combination of these classical models in sterile filtration of Immunoglobin G (IgG) and virus filtration of bovine serum albumin (BSA) led to better fit of the experimental data [13]. The idea is to combine the classical blocking models (i.e. combination of standard and intermediate models) and determine if a transition of fouling mechanisms exists during filtration. Originally, five combined blocking models were proposed: intermediate-standard, complete-standard, cake-standard, cake-intermediate and cake-complete models. The selection of candidates of combined blocking models was based on the values of n in the d^2t/dV^2 vs. dt/dV which suggest that the standard and intermediate models closely fit the experimental data. Moreover, the last four combined models were ignored because the blocking models other than the standard and intermediate models consistently yielded a poor fit of the data. Thus only the intermediate-standard model was considered for explaining the fouling mechanism of the filtration of pQR150 (20 kb) and pGEc47 (56 kb) plasmids DNA. Figure 5 shows the experimental result of the filtration test of pQR150 (20 kb) and pGEc47 (56 kb) at 5 and 8 psi transmembrane pressures and the corresponding best-fit lines for the intermediate-standard blocking model. The best fit of data occurred with the filtration of pGEc47 (56 kb) at 5 and 8 psi. Similar trends and levels of agreement between data and combined blocking model were observed with the other filtration tests.

Figure 5- Experimental data of filtrate volume vs. time fitted with the intermediate-standard blocking model. Solution containing 50 μg/ml of plasmid was filtered through 0.22 μm PVDF membrane. Figure 4a represents pQR150 (20 kb) at 5 psi, 4b) pQR150 (20 kb) at 8 psi, 4c) pGEc45 (56 kb) at 5 psi and 4d) pGEc47 (56 kb) at 8 psi transmembrane pressure.

Plasmid	Model	Standard error of estimates 5 psi transmembrane pressure	Standard error of estimates 8 psi transmembrane pressure
pQR150	Intermediate-standard	0.077	0.061
pGEc47	Intermediate-standard	0.035	0.165

Table 3 - The model fit errors of the filtration of pQR150 and pGEc47 at 5 and 8 psi transmembrane pressures.

Plasmid	5 psi transmembrane pressure		8 psi transmembrane pressure	
	k_{ic} (m^{-1})	k_s (m^{-1})	k_{ic} (m^{-1})	k_s (m^{-1})
pQR150	62.14	4.10	30.51	16.75
pGEc47	35.68	4.72	43.44	4.66

Table 4- The fouling parameters of the filtration of pQR150 and pGEc47 at 5 and 8 psi transmembrane pressures

The goodness of fit of the regression equations was again quantified by means of the standard error of estimate. Results in Table 3 show that the intermediate-standard model is the best model that described fouling during filtration of pQR150 (20 kb) and pGEc47 (56 kb) plasmids. Comparison with Table 2 shows that improvement of the goodness of fit is obtained by application of this combined blocking model. This suggests that the fouling process cannot be described as a single mechanism but as a combination of multiple fouling mechanisms. For future reference we have given Table 4, the best fit constants for the intermediate-standard models that describe the fouling in the four filtration experiments. The intermediate-standard blocking model is superior to the classical blocking model, i.e. the intermediate and standard blocking models as the model fit errors are smaller for the combined model.

## 3.5   Impact of fouling on transmission of plasmids DNA

Figures 6 and 7 describe the relationship between the dominant fouling mechanisms and plasmid transmission. The values of exponent n in Figure 3 were re-plotted in term of accumulated filtrate volume to simplify the analysis of fouling behaviour. This analysis is an attempt to correlate the mathematical analysis; which is applied to calculate the values of n, with the plasmid transmission data collected in the laboratory.

The transmission of both plasmids was high; >80 % during the filtration of the first 3.5 and 5.0 ml of filtrates for pQR150 (20 kb) and pGEc47 (56 kb) respectively (Figures 6a and 7a). However, a significant reduction of plasmid transmission was observed afterwards, with considerable differences for the filtration of pQR150 (20 kb) at 5 psi. The results also suggest that higher pressure filtration (at 8 psi) slightly increased the transmission of plasmids compared with the filtration operated at 5 psi before the significant drop of the transmission occurred. The observation is supported by the analysis by Hirasaki et al. (1995) that showed that the increased in transmembrane pressure assisted the penetration of plasmid molecule into the pore [27].

However, the operation at 8 psi increases the rate of fouling by increasing the flux towards the membrane. This is observed by rapid decline of filtrate flux during filtration at 8 psi compared with the filtration at 5 psi transmembrane pressure.
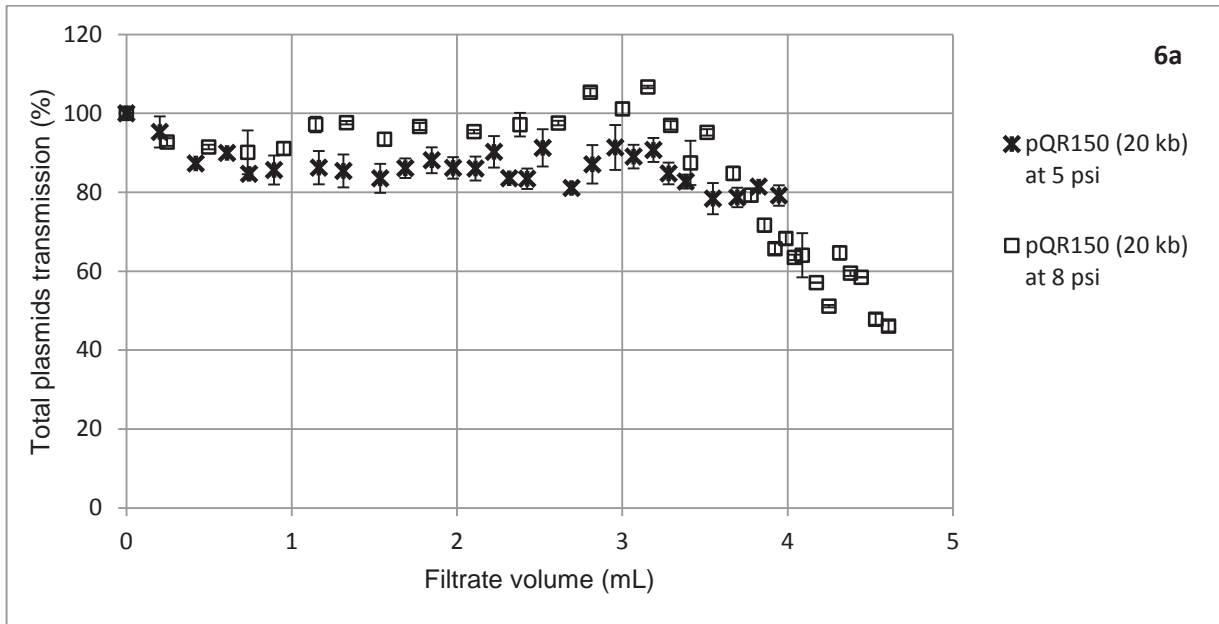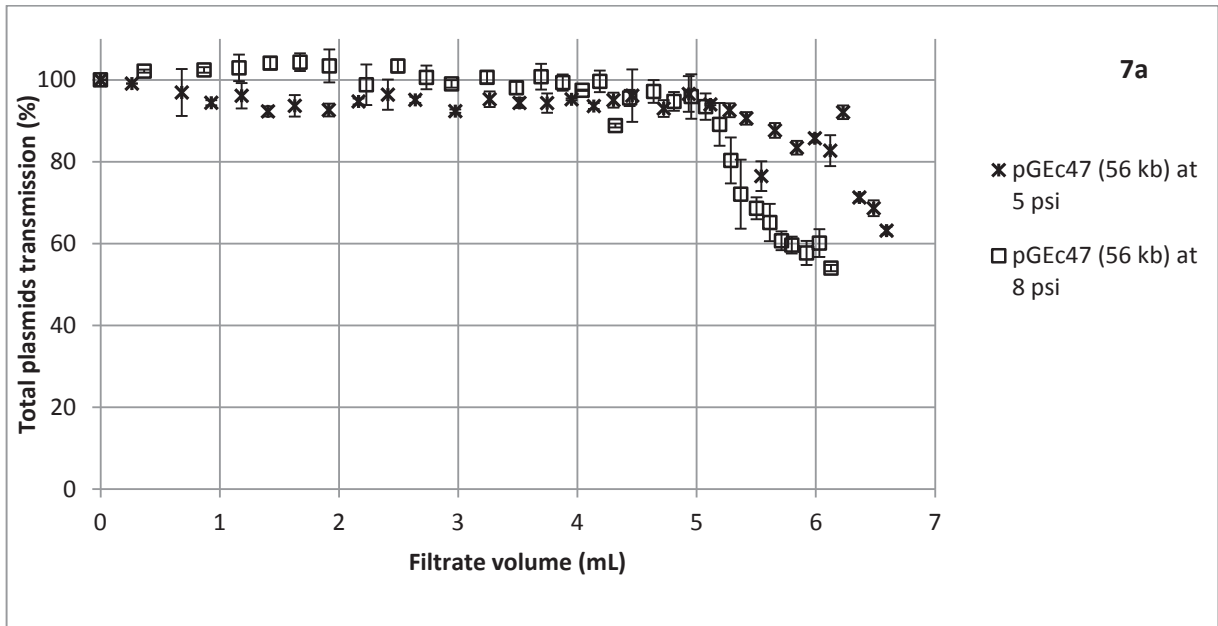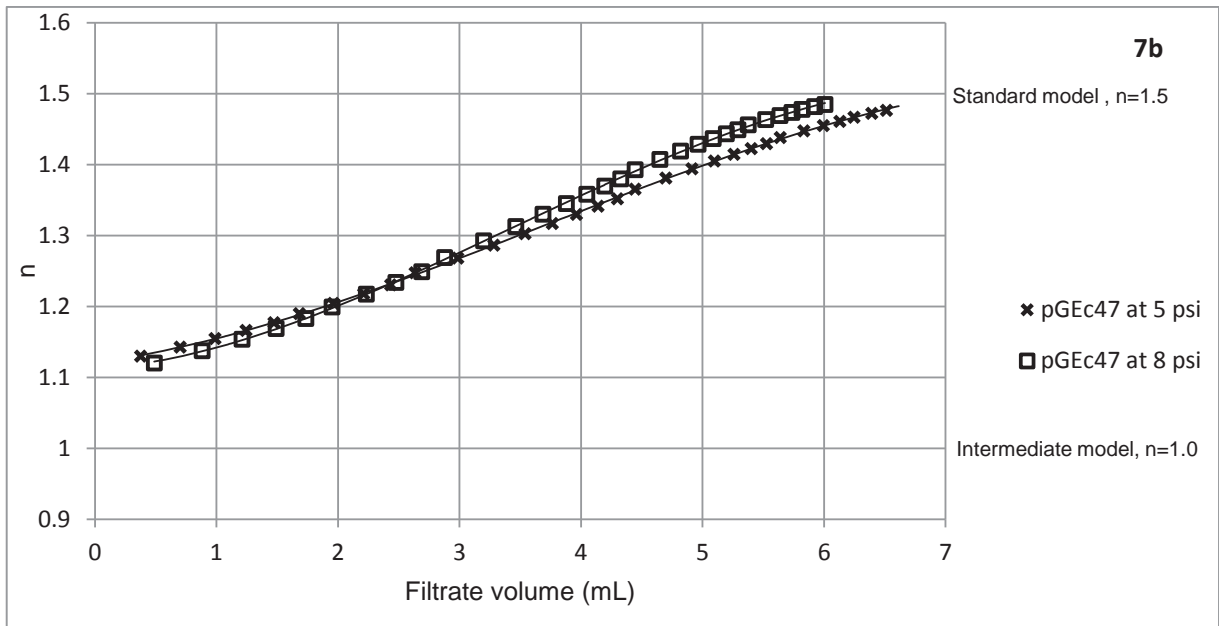
1
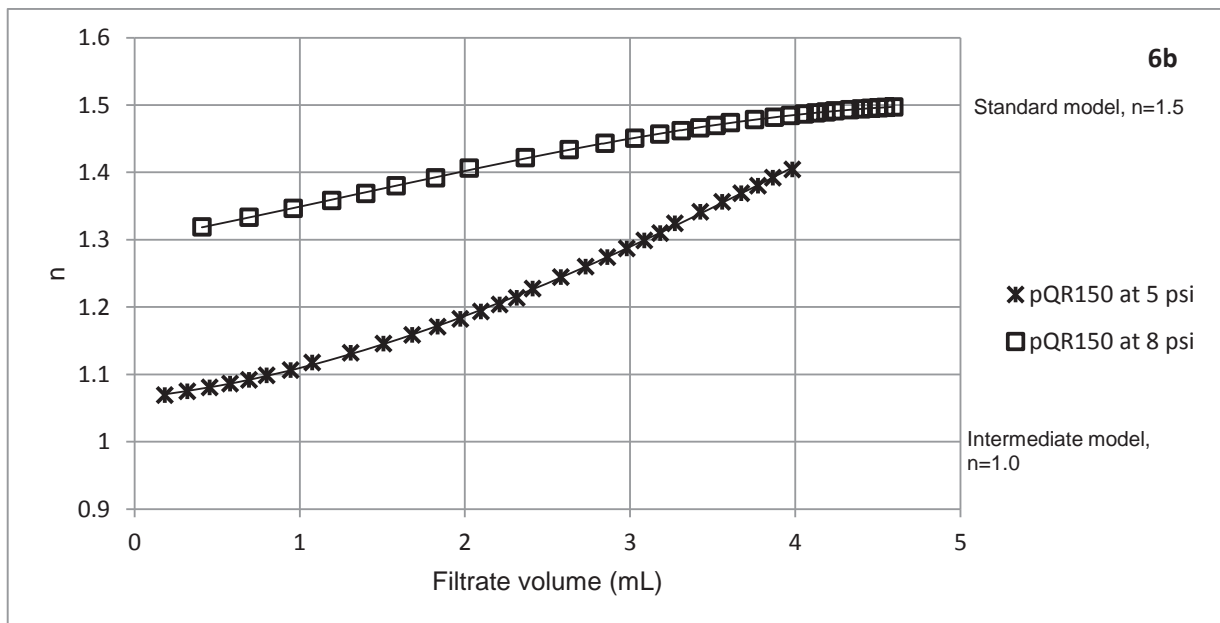
2

3   Figure 6- The transmission of pQR150 (20 kb) through 0.22 μm PVDF membranes at 5 and 8 psi

4   constant pressure filtration. The plasmids were collected in batches and the total transmission was

5   determined by the ratio of concentration of filtrate to the concentration of feed. Error bars in Fig 6a

6   indicate the standard deviation.

Figure 7- The transmission of pGEc47 (56 kb) through 0.22 μm PVDF membranes at 5 and 8 psi constant pressure filtration. The plasmids were collected in batches and the total transmission was determined by the ratio of concentration of filtrate to the concentration of feed. Error bars in Fig 7a indicate the standard deviation.

1   During the filtration of pQR150 at 8 psi, the transmission began to drop (after filtering ~3.7 ml

2   filtrates) during the point where the values of n= 1.48 which indicates that the blocking

3   mechanism tends to the standard blocking model (Figures 6a and 6b). The results suggested

4   that at this point, internal fouling started to dominate the filtration and influenced the reduction of

5   internal pore diameters and consequently reduced the transmission of plasmids.

6   Similar trends were observed during the filtration of pGEc47 at 5 and 8 psi (Figures 7a and 7b).

7   The reduction of plasmid transmission can be correlated with the values of n in d^2t/dV^2 vs. dt/dV

8   plot. During the time when the transmission started to drop at 5 and 8 psi filtration, the values of

9   n were detected at ~1.43 and ~1.44 respectively. Again, the significant reduction of plasmids

10 transmission correlated with the values of n approaching 1.5.

11 The analysis of the trend of n vs. filtrate volume, in term of molecular weight shows that the drop

12 of plasmid DNA transmission during 8 psi transmembrane pressure filtration occurred at a

13 smaller volume for pQR150 (20 kb), i.e. 3.5 ml, whereas for pGEc47 (56 kb), the drop of

14 transmission occurred at a higher filtrate volume of 5 ml. The trend can be correlated with the

15 evolution of n values which is for pGEc47 plasmid, the value of n= 1.5 was obtained after ~ 6 ml

16 of filtrate is collected, compared with the pQR150 which is around ~4 ml. The results suggest

17 that the constriction of membrane pores by plasmid as explained by standard model (n=1.5)

18 caused the drop in the plasmid transmission. The constriction of the pore throat influences the

19 deformation and elongation of plasmid; which is the critical characteristics of the molecule to

20 penetrate the pore. The results also suggest that besides the molecular weight [29], the

21 transmission is also influenced by the dominant fouling mechanism of DNA.

22 It is interesting to note that the transmission of plasmid DNA reduced significantly when the pore

23 constriction blocking mechanism (standard model) dominated the fouling of the membrane.

During the initial stage of filtration when the fouling was dominated by the intermediate blocking mechanism, the blockage was caused by the superposition of plasmids that are trapped on the surface of membrane. However, the transmission of plasmids began to decrease strongly when the pore constriction mechanism started to dominate the fouling. At this stage, the reduction of pore size due to the internal fouling influenced the flexibility and ability of plasmid to penetrate the pore. Constriction of the internal pore structure would reduce the available space for plasmid trajectory. Plasmid is a negatively charge molecule and at high fluid concentration; when the space between plasmid molecules is reduced, electrostatic repulsion between molecules is increased. The repulsion increases the rigidity of plasmids and will influence its trajectory through the membrane. During the initial stage of filtration when high transmission of plasmids was observed, the higher magnitudes of the shear and elongational stresses that occur at elevated transmembrane pressure (8 psi) can overcome this electrostatic repulsion and consequently increase the flexibility of the plasmid. High flexibility of plasmid assists the penetration of this molecule into pores. This hypothesis is in agreement with the transmission data of pQR150 (20 kb) and pGEc47 (56 kb) plasmids where the transmission was higher at 8 psi compared with 5 psi transmembrane pressure during the initial stage of filtration. In contrast, low transmembrane pressure encourages the retention of DNA at the surface of membrane. This is probably due to low velocity magnitude that gives rise to slower trajectory of plasmids leading to the entrapment of these molecules inside the membrane.

The data presented is also in agreement with Morao et al. (2011) which explained that the charged effect plays critical role in plasmid transmission during filtration. The authors describe that the excessive accumulation of DNA molecule on the surface of membrane imparts negatively charge monolayer of plasmid which reject the trajectory of other plasmid molecules near the pores [30].

The fouling of plasmid DNA as captured by the blocking models and filtration law can be validated using various microscopy techniques. We intend to highlight this issue in a manuscript that discusses the direct visualisation of plasmid DNA fouling.

4 Conclusions

Interestingly, the combined intermediate-standard model can be applied to describe the flux decline behaviour of the filtration of large plasmid DNA even though the model was originally developed to explain the filtration behaviour of rigid spherical particles. This work has demonstrated that the model can also play a practical role in explaining the fouling behaviour inside polymeric membrane that contains complex interconnected pores in spite of the assumption of the model that describes the membrane as parallel arrays of cylindrical pore.

During the filtration of both pQR150 and pGEc47 plasmids at 5 and 8 psi transmembrane pressures, it was found that the intermediate blocking model dominated the fouling during short initial filtration period (except for filtration of pQR150 at 8 psi). The standard blocking mechanism subsequently dominated the fouling for the remainder of the filtration.

The transmission of plasmids dropped significantly at a point when $n\sim1.5$ in Equation 1 during the filtration at higher transmembrane pressure (at 8 psi compared with filtration at 5 psi). It is thought that high transmembrane pressure influenced the retention of plasmid by capturing this molecule inside the membrane. It is also interesting to note that the decreased of plasmid transmission is due to the internal fouling as suggested in d^2t/dV^2 *vs. dt/dV* plots. In summary, previous work reported in the literature has shown that membrane fouling due to smaller molecules (proteins or small plasmids) can be captured successfully with classical blocking models. Our work stresses the possibility of a more complex fouling behaviour during sterile filtration of larger plasmids due to their flexible nature.

Nomenclature

A_0	Initial membrane frontal area	m^2
k_b	Complete blocking constant	s^{-1}
k_c	Cake filtration blocking constant	sm^{-6}
k_i	Intermediate blocking constant	m^{-3}
k_{ic}	Intermediate blocking constant in combined model	m^{-1}
k_s	Standard blocking constant	m^{-1}
t	Filtration time	S
V	Filtrate volume	m^3
V_0	Initial volumetric flow rate	m^3/s
V_{max}	Maximum volumetric capacity of membrane per unit area	m^3/m^2

Acknowledgements

References

1. Liu, M.A., *Immunologic Basis of Vaccine Vectors.* Immunity, 2010. **33**(4): p. 504-515.

2. Prather, K.J., et al., *Industrial scale production of plasmid DNA for vaccine and gene therapy: plasmid design, production, and purification.* Enzyme and Microbial Technology, 2003. **33**(7): p. 865-883.

3. Prazeres, D.M.F. and G.N.M. Ferreira, *Design of flowsheets for the recovery and purification of plasmids for gene therapy and DNA vaccintion.* Chemical Engineering and Processing: Process Intensification, 2004. **43**(5): p. 609-624.

4. Levy, M.S., et al., *Biochemical engineering approaches to the challenges of producing pure plasmid DNA.* Trends in Biotechnology, 2000. **18**(7): p. 296-305.

5.	Shamlou, P.A., *Scaleable processes for the manufacture of therapeutic quantities of plasmid DNA.* Biotechnology and Applied Biochemistry, 2003. **37**(3): p. 207-218.

6.	Carnes, A.E. and J.A. Williams, *Plasmid DNA Manufacturing Technology.* Recent Patents on Biotechnology, 2007. **1**(2): p. 151-166.

7.	Kong, S., J. Aucamp, and N.J. Titchener-Hooker, *Studies on membrane sterile filtration of plasmid DNA using an automated multiwell technique.* Journal of Membrane Science, 2010. **353**(1-2): p. 144-150.

8.	Levy, M.S., et al., *Effect of shear on plasmid DNA in solution.* Bioprocess and Biosystems Engineering, 1999. **20**(1): p. 7-13.

9.	Bakhshayeshi, M., et al., *Use of confocal scanning laser microscopy to study virus retention during virus filtration.* Journal of Membrane Science, 2011. **379**(1-2): p. 260-267.

10.	Ferrando, M., et al., *An approach to membrane fouling characterization by confocal scanning laser microscopy.* Journal of Membrane Science, 2005. **250**(1-2): p. 283-293.

11.	Zeman, L., *Characterization of microfiltration membranes by image analysis of electron micrographs.: Part II. Functional and morphological parameters.* Journal of Membrane Science, 1992. **71**(3): p. 233-246.

12.	Hermia, J., *Constant pressure blocking filtration laws-application to power law non-Newtonian fluids.* Chemical Engineering Research and Design, 1982. **60a**: p. 183-187.

13.	Bolton, G., D. LaCasse, and R. Kuriyel, *Combined models of membrane fouling: Development and application to microfiltration and ultrafiltration of biological fluids.* Journal of Membrane Science, 2006. **277**(1-2): p. 75-84.

14.	Ho, C.-C. and A.L. Zydney, *A Combined Pore Blockage and Cake Filtration Model for Protein Fouling during Microfiltration.* Journal of Colloid and Interface Science, 2000. **232**(2): p. 389-399.

15.	Zydney, A.L. and C.-C. Ho, *Scale-up of microfiltration systems: fouling phenomena and Vmax analysis.* Desalination, 2002. **146**(1-3): p. 75-81.

16.	Laska, M.E., et al., *Robust scale-up of dead end filtration: Impact of filter fouling mechanisms and flow distribution.* Biotechnology and Bioengineering, 2005. **92**(3): p. 308-320.

17.	Iritani, E., et al., *Flux decline behavior in dead-end microfiltration of protein solutions.* Journal of Membrane Science, 1995. **103**(1–2): p. 181-191.

18.	Bowen, W.R., J.I. Calvo, and A. Hernández, *Steps of membrane blocking in flux decline during protein microfiltration.* Journal of Membrane Science, 1995. **101**(1–2): p. 153-165.

1 19. Rajniak, P., et al., *Sterilizing filtration--Principles and practice for successful scale-up to*
2 *manufacturing.* Journal of Membrane Science, 2008. **325**(1): p. 223-237.

3 20. Haber, C., et al., *Membrane chromatography of DNA: Conformation-induced capacity and*
4 *selectivity.* Biotechnology and Bioengineering, 2004. **88**(1): p. 26-34.

5 21. Larson, J.W., et al., *Single DNA molecule stretching in sudden mixed shear and elongational*
6 *microflows.* Lab on Chip, 2006. **6**: p. 1187.

7 22. Wubbolts, M.G., O. Favre-Bulle, and B. Witholt, *Biosynthesis of synthons in two-liquid-phase*
8 *media.* Biotechnology and Bioengineering, 1996. **52**(2): p. 301-308.

9 23. Kim, M.-m. and A.L. Zydney, *Particle-particle interactions during normal flow filtration: Model*
10 *simulations.* Chemical Engineering Science, 2005. **60**(15): p. 4073-4082.

11 24. Tracey, E.M. and R.H. Davis, *Protein Fouling of Track-Etched Polycarbonate Microfiltration*
12 *Membranes.* Journal of Colloid and Interface Science, 1994. **167**(1): p. 104-116.

13 25. Bowen, W.R. and Q. Gan, *Properties of microfiltration membranes: Flux loss during constant*
14 *pressure permeation of bovine serum albumin.* Biotechnology and Bioengineering, 1991. **38**(7):
15 p. 688-696.

16 26. Kelly, S.T., W. Senyo Opong, and A.L. Zydney, *The influence of protein aggregates on the fouling*
17 *of microfiltration membranes during stirred cell filtration.* Journal of Membrane Science, 1993.
18 **80**(1): p. 175-187.

19 27. Hirasaki, T., et al., *Permeation mechanism of DNA molecules in solution through cuprammonium*
20 *regenerated cellulose hollow fiber (BMMtm).* Journal of Membrane Science, 1995. **106**(1-2): p.
21 123-129.

22 28. Watson, M.P., et al., *Sterilizing filtration of plasmid DNA: Effects of plasmid concentration,*
23 *molecular weight, and conformation.* Biotechnology Progress, 2006. **22**(2): p. 465-470.

24 29. Kong, S., N. Titchener-Hooker, and M.S. Levy, *Plasmid DNA processing for gene therapy and*
25 *vaccination: Studies on the membrane sterilisation filtration step.* Journal of Membrane Science,
26 2006. **280**(1-2): p. 824-831.

27 30. Morão, A.M., et al., *Ultrafiltration of supercoiled plasmid DNA: Modeling and application.*
28 Journal of Membrane Science, 2011. **378**(1-2): p. 280-289.

29

30

N2 Feeder

V1

P1
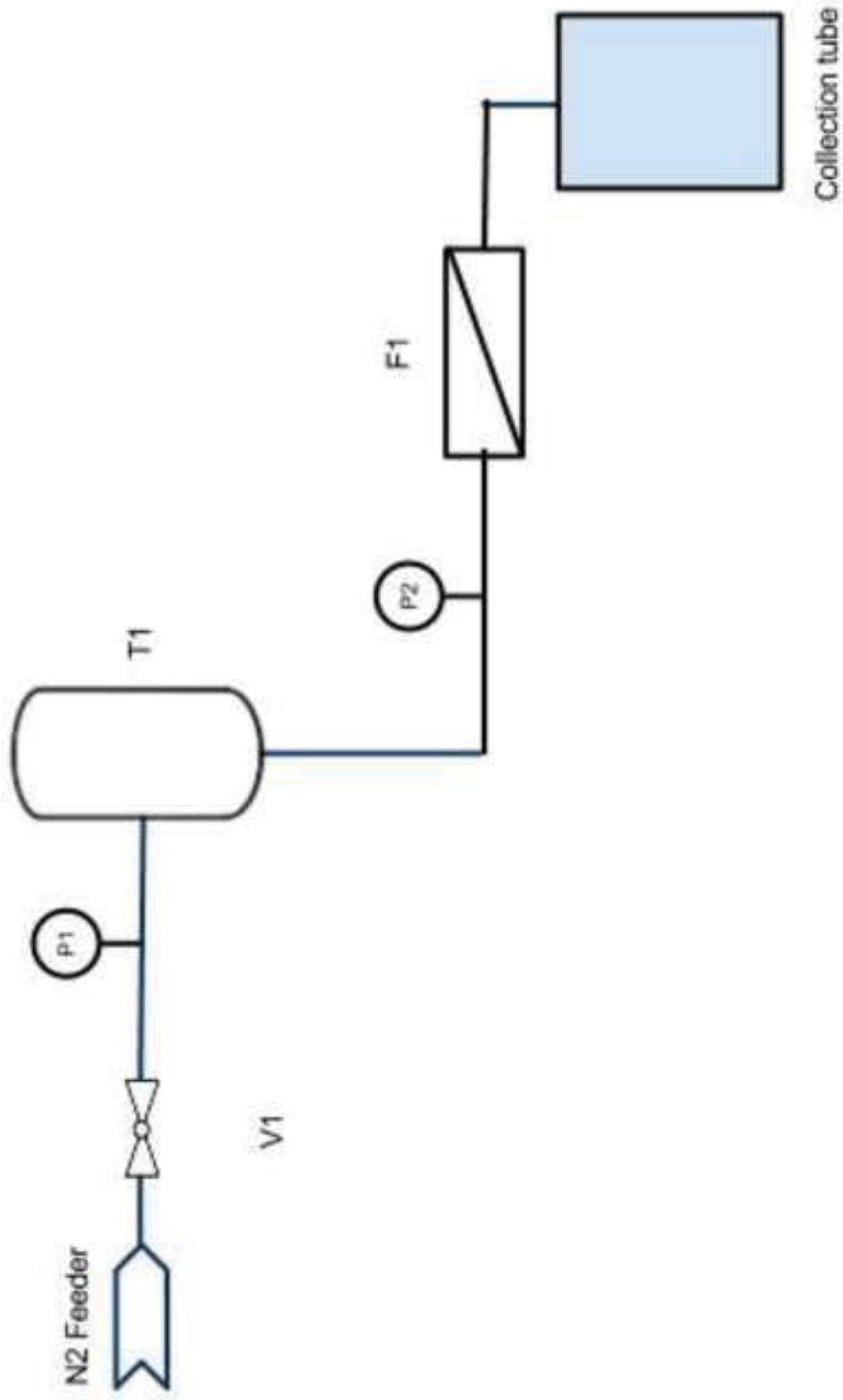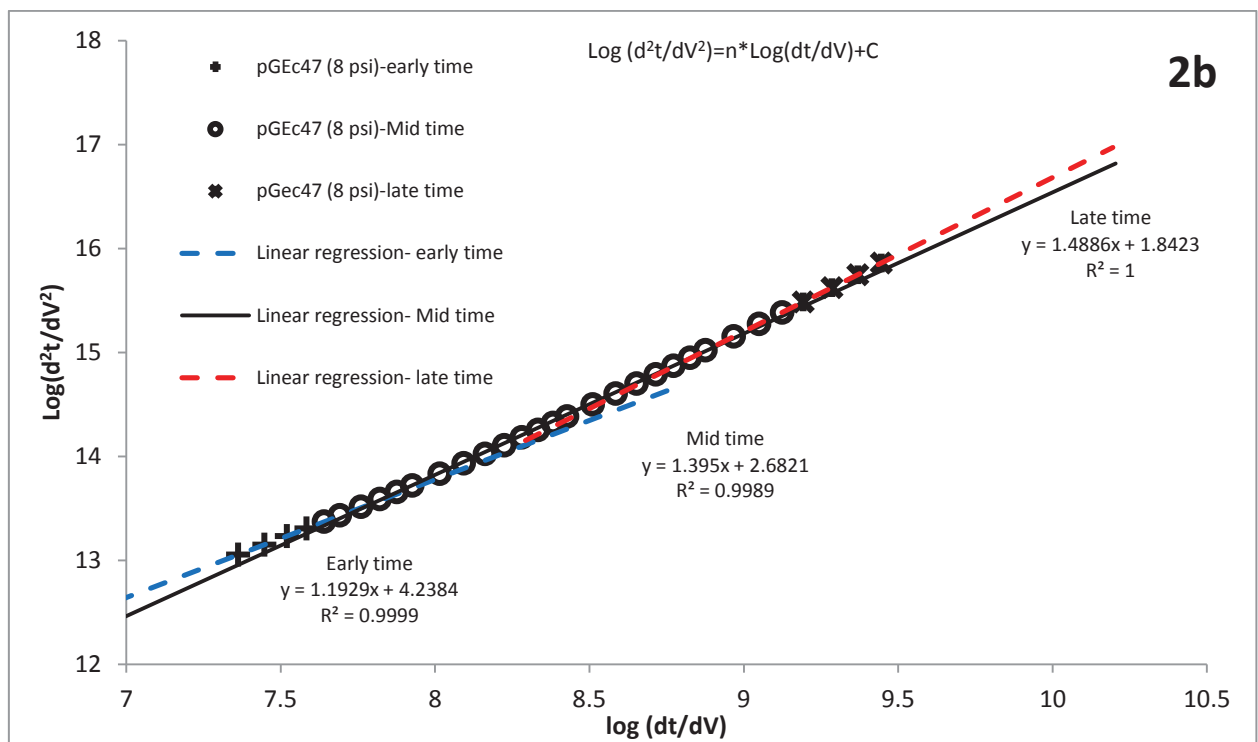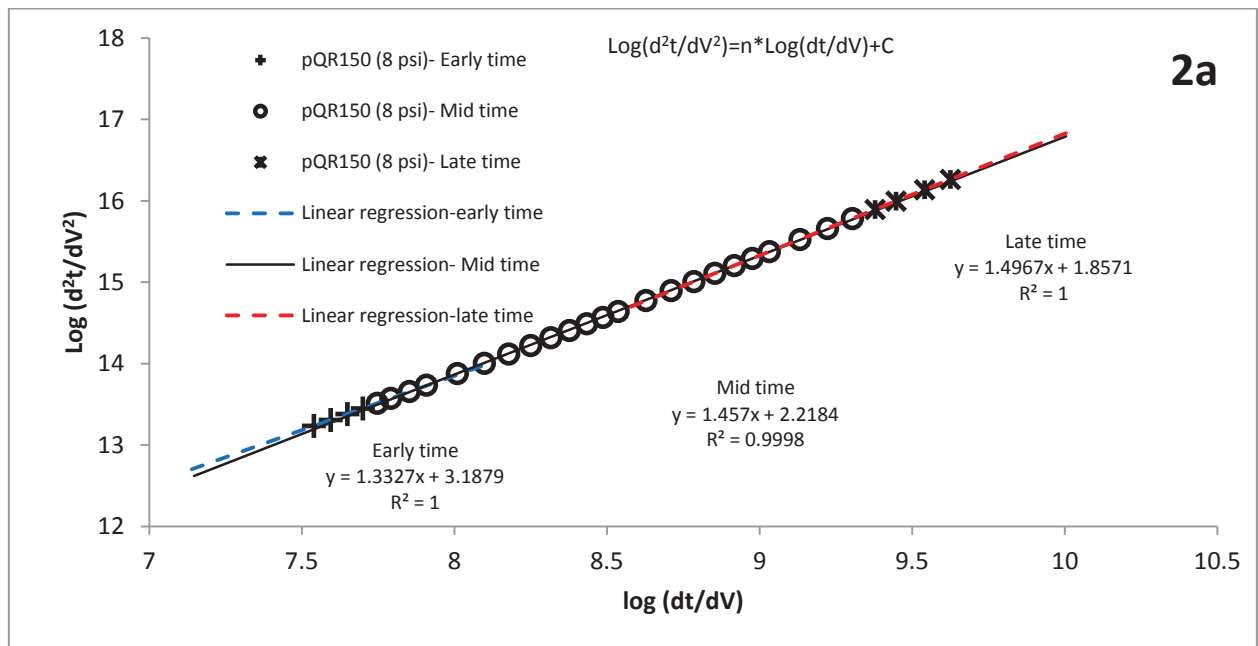
T1

P2

F1

Collection tube

Figure 2

Figure 1- Flux decline analysis of pQR150 (20 kb) and pGEc47 (56 kb) filtrations at 8 psi transmembrane pressure.
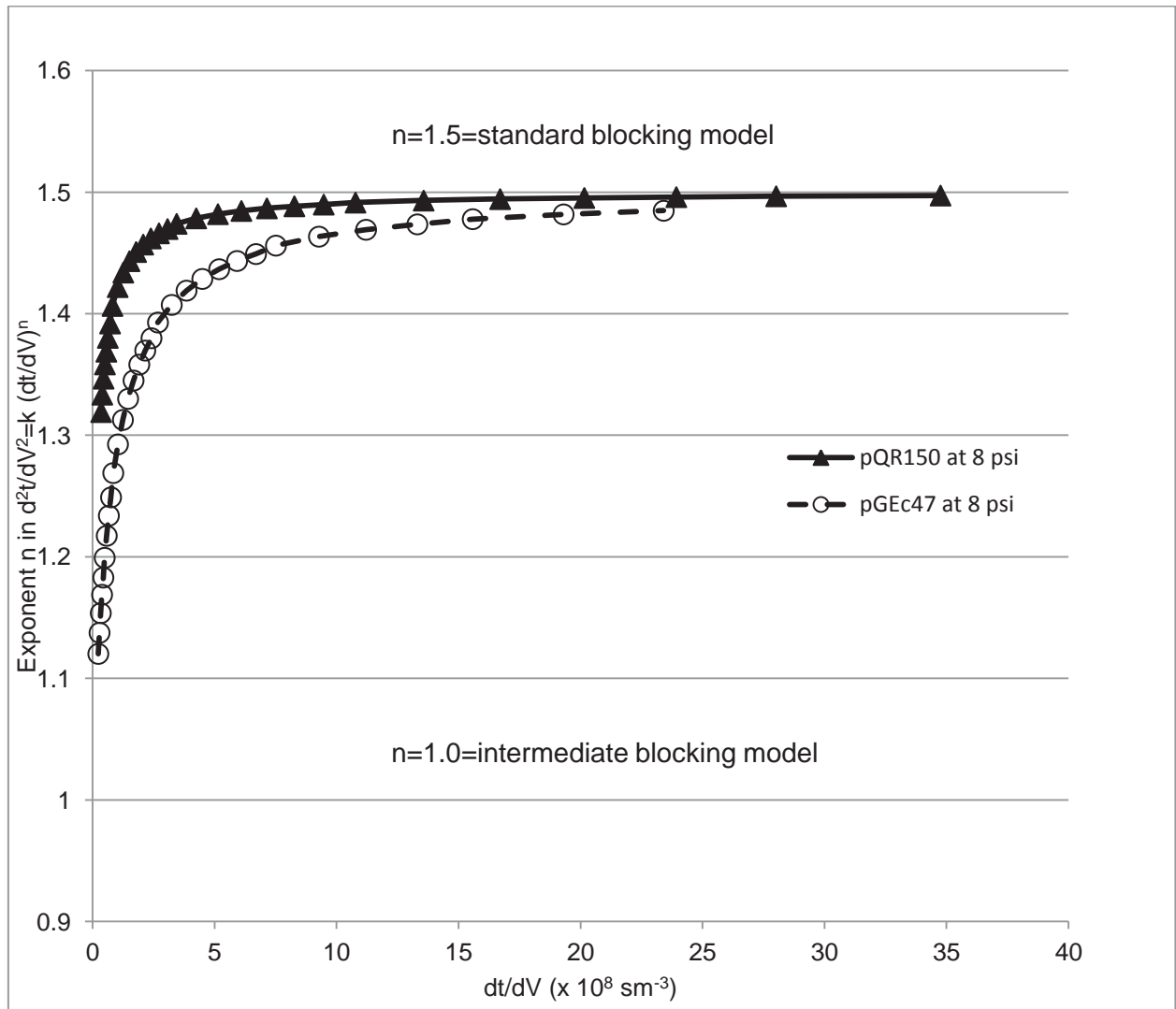
Figure 3

Figure 1 - The plot of exponent *n* (Equation 1) vs. *dt/dV* of the filtration of pQR150 (20 kb) and pGEc47

(56 kb) at 8 psi transmembrane pressure.

Figure 4
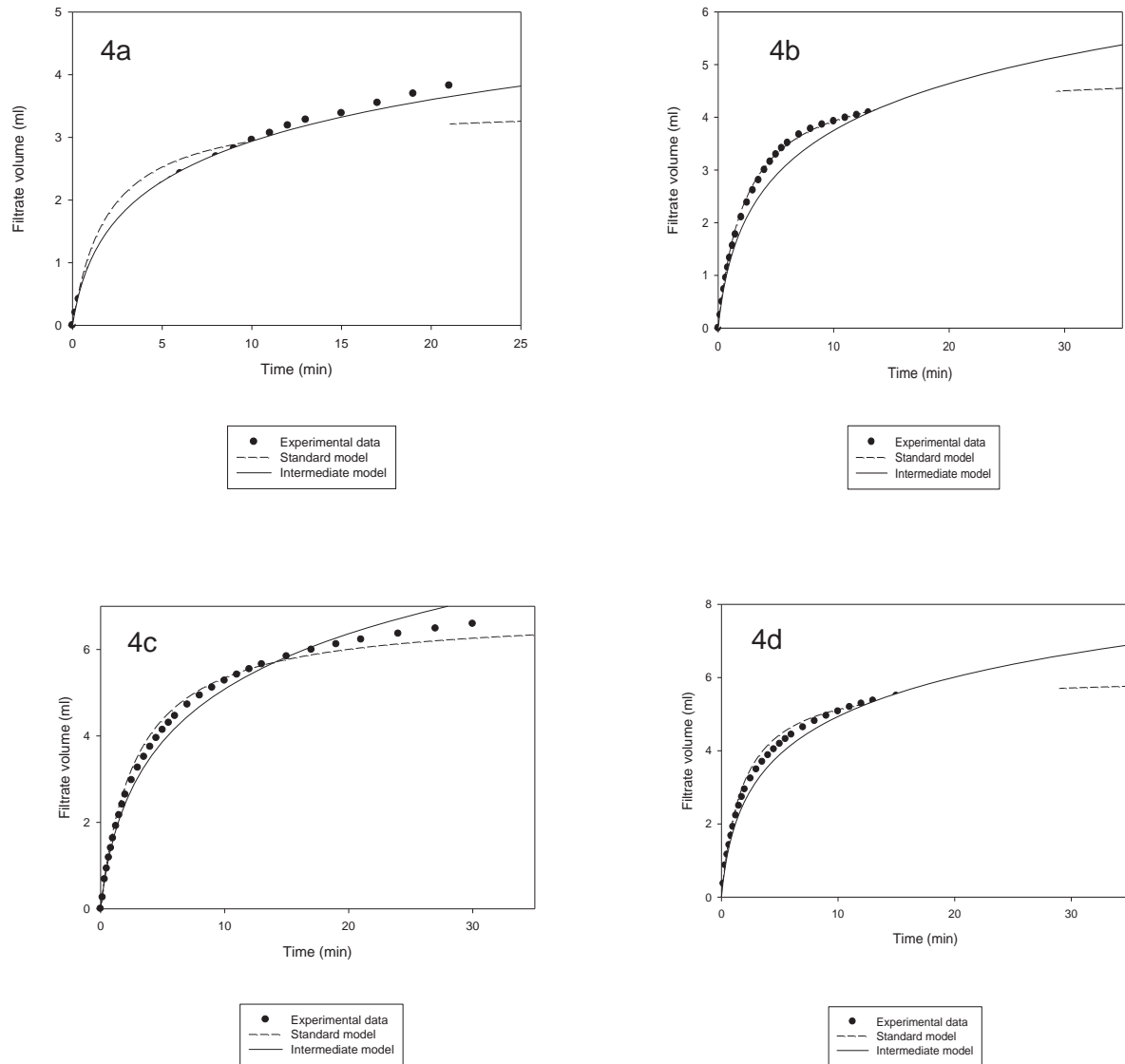

Figure 1 - Experimental data of filtrate volume vs. time fitted with the standard and intermediate blocking models. Solution containing 50 µg/ml of plasmid was filtered through 0.22 µm PVDF membrane. Figure 4a represents pQR150 (20 kb) at 5 psi, 4b) pQR150 (20 kb) at 8 psi, 4c) pGEc45 (56 kb) at 5 psi and 4d) pGEc47 (56 kb) at 8 psi transmembrane pressure.
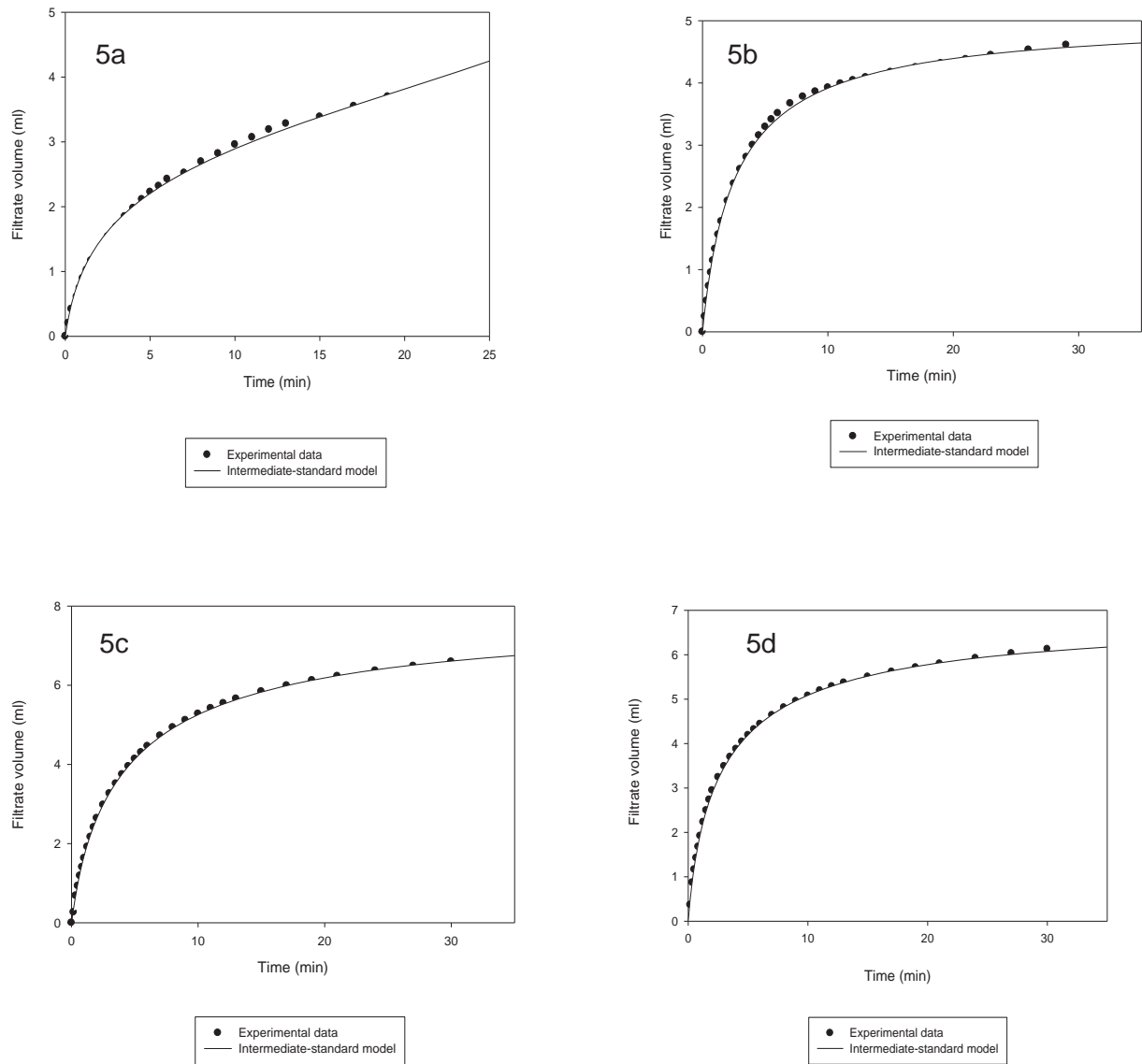
Figure 5

Figure 1- Experimental data of filtrate volume vs. time fitted with the intermediate-standard blocking model. Solution containing 50 µg/ml of plasmid was filtered through 0.22 µm PVDF membrane. Figure 4a represents pQR150 (20 kb) at 5 psi, 4b) pQR150 (20 kb) at 8 psi, 4c) pGEc45 (56 kb) at 5 psi and 4d) pGEc47 (56 kb) at 8 psi transmembrane pressure.
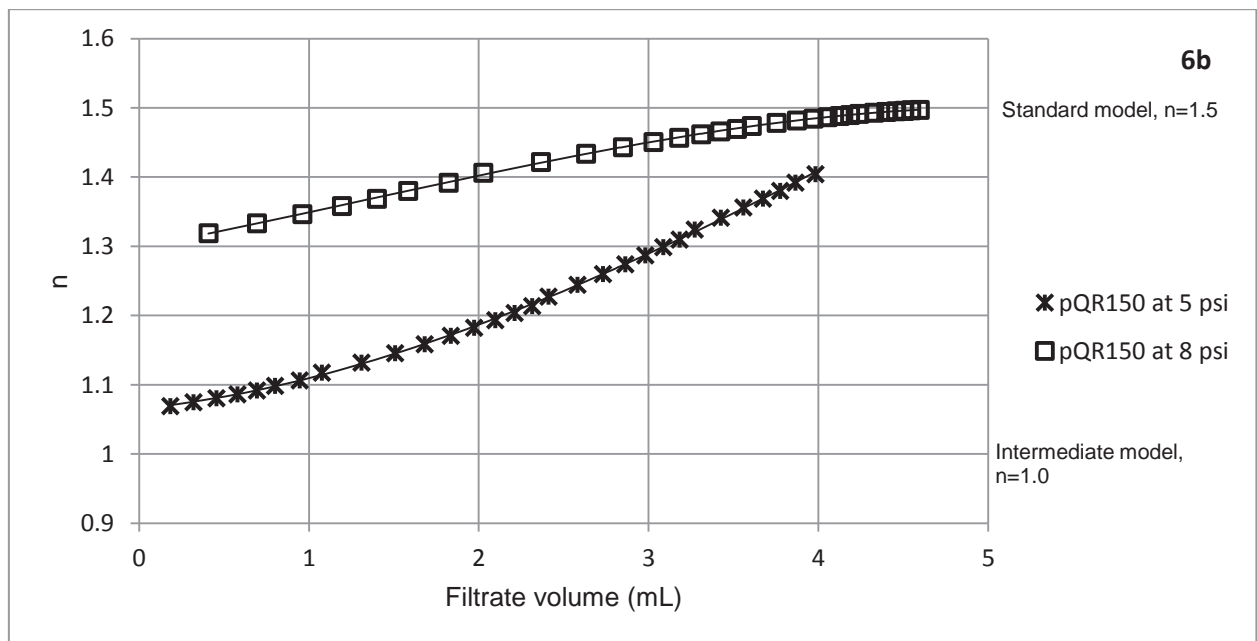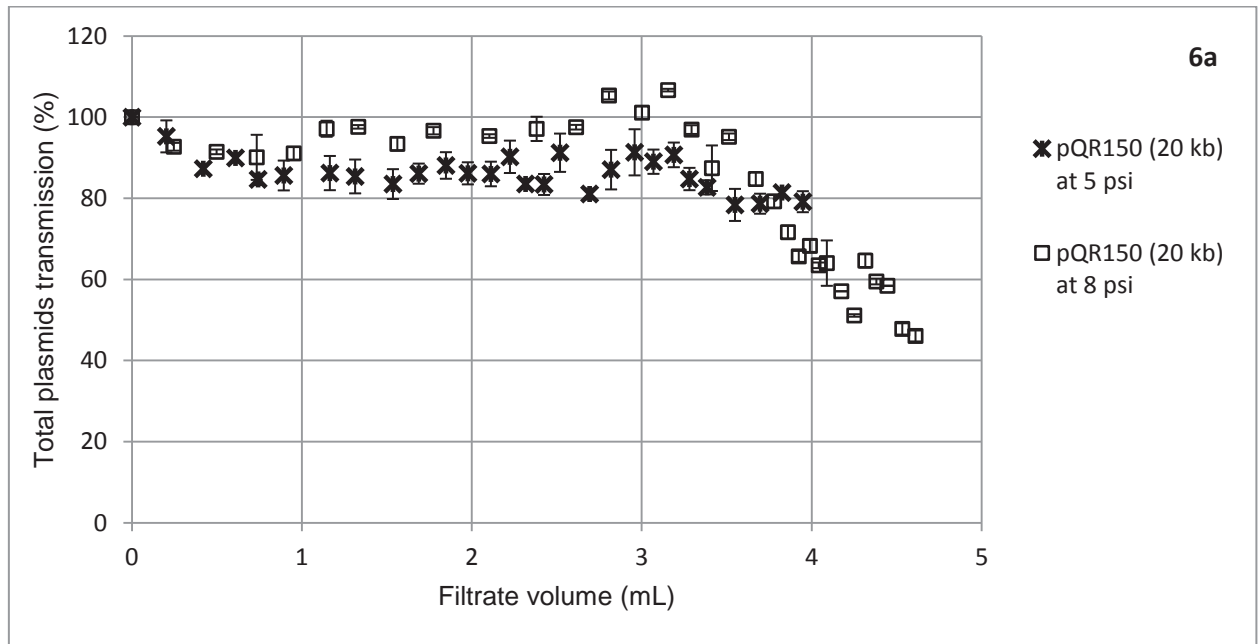
Figure 6

Figure 1- The transmission of pQR150 (20 kb) through 0.22 μm PVDF membranes at 5 and 8 psi constant pressure filtration. The plasmids were collected in batches and the total transmission was determined by the ratio of concentration of filtrate to the concentration of feed. Error bars in Fig 6a indicate the standard deviation.
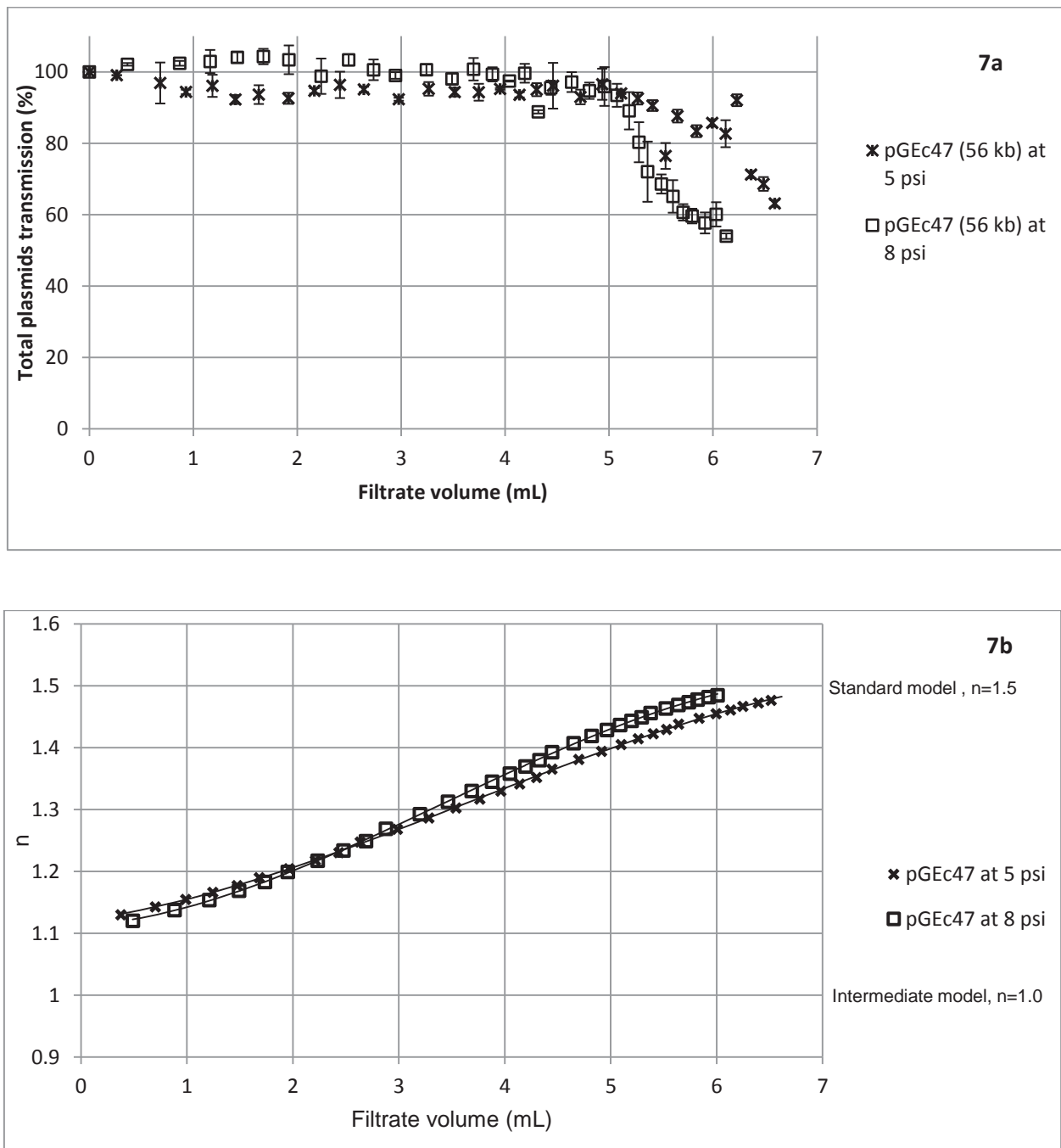
Figure 7

7a

7b

Figure 1- The transmission of pGEc47 (56 kb) through 0.22 μm PVDF membranes at 5 and 8 psi constant pressure filtration. The plasmids were collected in batches and the total transmission was determined by the ratio of concentration of filtrate to the concentration of feed. Error bars in Fig 7a indicate the standard deviation.

Table 1

Models	Equations	Fouling parameter
Standard blocking [16]	$V = (V_0 t)\left(1 + \dfrac{k_s V_0}{A_0} t\right)^{-1}$	$k_s\ (\text{m}^{-1})$
Intermediate blocking [16]	$V = \dfrac{1}{k_i} \ln(1 + k_i V_0 t)$	$k_i\ (\text{m}^{-3})$
Complete blocking [16]	$V = \dfrac{V_0}{k_b}\left[1 - \exp(-k_b t)\right]$	$k_b\ (\text{s}^{-1})$
Cake filtration [16]	$V = \dfrac{1}{V_0 k_c}\left(\sqrt{1 + (2 k_c V_0^2 t)} - 1\right)$	$k_c\ (\text{s.m}^{-6})$
Intermediate-standard [13]	$V = \dfrac{A_0}{k_{ic}} \ln\left(1 + \dfrac{2 k_{ic}(V_0/A_0)t}{2 + k_s(V_0/A_0)t}\right)$	$k_{ic}\ (\text{m}^{-1})$ and $k_s\ (\text{m}^{-1})$
Complete-standard [13]	$V = \dfrac{V_0}{k_b}\left(1 - \exp\left(\dfrac{-2 k_b t}{2 + k_s(V_0/A_0)t}\right)\right)$	$k_b\ (\text{s}^{-1})$ and $k_s\ (\text{m}^{-1})$

Table 1- Summary of classical and combined blocking models for constant transmembrane pressure filtration

Table 2

Plasmid	Model	Standard error of estimates	Standard error of estimates
		5psi transmembrane pressure	8psi transmembrane pressure
pQR150	Standard	0.325	0.078
	Intermediate	0.120	0.272
pGEc47	Standard	0.191	0.342
	Intermediate	0.221	0.198

Table 1 - Standard error of estimates of the filtration of pQR150 (20 kb) and pGEc47 (56 kb) at 5 and 8 psi.

Table 3

Plasmid	Model	Standard error of estimates	Standard error of estimates
		5 psi transmembrane pressure	8 psi transmembrane pressure
pQR150	Intermediate-standard	0.077	0.061
pGEc47	Intermediate-standard	0.035	0.165

Table 1 - The model fit errors of the filtration of pQR150 and pGEc47 at 5 and 8 psi transmembrane pressures.

Table 4

Plasmid	5 psi transmembrane pressure		8 psi transmembrane pressure	
	k_{ic} (m^{-1})	k_s (m^{-1})	k_{ic} (m^{-1})	k_s (m^{-1})
pQR150	62.14	4.10	30.51	16.75
pGEc47	35.68	4.72	43.44	4.66

Table 1- The fouling parameters of the filtration of pQR150 and pGEc47 at 5 and 8 psi transmembrane pressures